Inorganic Chemistry

Article

pubs.acs.org/IC

Variable Framework Structures and Centricities in Alkali Metal Yttrium Selenites, $AY(SeO_3)_2$ (A = Na, K, Rb, and Cs)

Seong-eun Bang, Dong Woo Lee, and Kang Min Ok*

Department of Chemistry, Chung-Ang University, 84 Heukseok-ro, Dongjak-gu, Seoul 156-756, Republic of Korea

Supporting Information

ABSTRACT: Pure samples of a series of yttrium selenites, $AY(SeO_3)_2$ (A = Na, K, Rb, and Cs), were prepared through hydrothermal reactions using A_2CO_3, $Y(NO_3)_3{\cdot}6H_2O$, and SeO_2. All four materials have 3D framework structures; however, they exhibit different channel geometries. The three-dimensional framework of $NaY(SeO_3)_2$ consists of zigzag chains of vertex-shared YO_7 polyhedra and SeO_3 linkers. $KY(SeO_3)_2$ and $RbY(SeO_3)_2$ reveal channels composed of corner-shared YO_6 octahedra and SeO_3 polyhedra. $CsY(SeO_3)_2$ exhibits a highly symmetric cage structure with radially spreading linkages of YO_6 and SeO_3 groups. Close structural examinations suggest that the cation size and coordination environment significantly influence the backbone architectures and their centricities. Second-harmonic generation (SHG) measurements on the powder sample of $NaY(SeO_3)_2$ reveal that the NCS selenite possesses a similar SHG efficiency to that of $NH_4H_2PO_4$ (ADP).

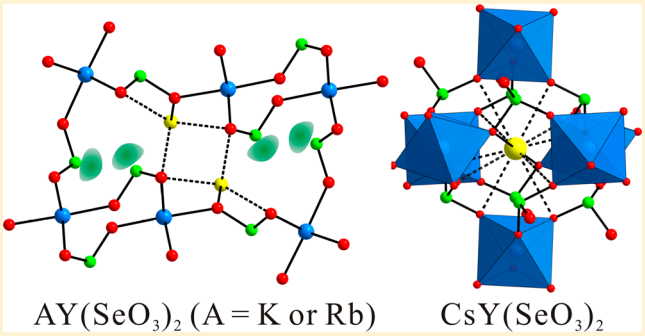

INTRODUCTION

Mixed metal selenites, i.e., oxides accommodating a Se^{4+} with other metal cations, have drawn tremendous attention attributable to their synthetic and structural adaptabilities. One of the most commonly utilized starting materials in the synthetic solid-state reactions for selenites is selenium dioxide (SeO_2). With such an excellent reactivity with other oxides as well as a low triple point (340 °C), SeO_2 is widely employed as a flux for the growth of novel mixed metal oxide crystals at lower temperatures.[1−3] In addition, SeO_2 reveals a very good water-solubility; a portion of 264 g of solid SeO_2 can be dissolved in 100 g of water at 22 °C,[1] which makes the material an excellent starting compound in hydrothermal reactions. Moreover, the coordination environment of the Se^{4+} cation is of particular interest. The Se^{4+} cation generally exhibits an asymmetric SeO_3 trigonal pyramidal moiety with a stereoactive lone pair in oxide materials. Once the SeO_3 groups are combined with other polyhedra such as octahedra or tetrahedra, a great deal of framework flexibilities could be possible.[4−12] The local asymmetric coordination moieties in SeO_3 groups often effectively generate macroscopic non-centrosymmetry (NCS) in the combined materials. In fact, discovering the NCS materials is extremely important due to their scientifically and industrially important materials' characteristics such as piezoelectricity, ferroelectricity, second-harmonic generation (SHG), and pyroelectricity.[13−16] Thus, huge efforts have been made to find superior performing NCS materials. A few successful approaches include combining the cations with second-order Jahn−Teller distortion (d^0 transition metals and lone pair cations),[17−23] d^{10} transition metal cations,[8,24,25] and borates with asymmetric π systems during the syntheses.[26−28] However, when the asymmetric groups are arranged in an antiparallel manner, materials with extended structures often tend to crystallize in centrosymmetric (CS) structures. Thus, to design new functional asymmetric materials rationally, it is very important to have fundamental knowledge regarding the essential elements that influence the macroscopic centricities. Several reported factors affecting the materials' centricities are the hydrogen-bonding, the size of constituent cations, and the flexible coordination.[11,22,29−34] While we systematically investigated the A^+−Y^{3+}−Se^{4+}−oxide (A = alkali metals) system, we found four stoichiometrically equivalent quaternary alkali metal yttrium selenium oxides. Although many yttrium selenites have been discovered, only a few quaternary yttrium selenium oxides materials have been reported thus far.[23,35−38] Among them, $NaY(SeO_3)_2$,[35] $Y(HSeO_3)(SeO_3)(H_2O){\cdot}H_2O$,[36] and $YVSe_2O_8$[23] reveal NCS space groups. We introduce herein high yield synthesis and thorough property measurements of a series of novel selenites, $AY(SeO_3)_2$ (A = Cs, Rb, K, and Na). We will present the dimension and the coordination environment of alkali metals playing key roles in shaping channel structures and the overall centricities in the reported materials.

EXPERIMENTAL SECTION

Reagents. Na_2CO_3 (Hayashi, 99.5%), K_2CO_3 (Jin Chemical, 99.5%), Rb_2CO_3 (Acros, 99.0%), Cs_2CO_3 (Aldrich, 99.0%), SeO_2

Received: March 10, 2014
Published: April 22, 2014

   dx.doi.org/10.1021/ic500548v | Inorg. Chem. 2014, 53, 4756−4762

(Aldrich, 98.0%), and $Y(NO_3)_3{\cdot}6H_2O$ (Alfa Aesar, 99.9%) were employed as received.

Synthesis. Phase pure single crystals for all the reported materials were grown by hydrothermal reactions. With $AY(SeO_3)_2$ (A = Na, K, Rb, or Cs), 4.00×10^{-3} mol of A_2CO_3, 1.00×10^{-3} mol (0.383 g) of $Y(NO_3)_3{\cdot}6H_2O$, 4.00×10^{-3} mol (0.444 g) of SeO_2, and 5 mL [7 mL for $CsY(SeO_3)_2$] of water were mixed. The separate reaction mixtures were introduced into autoclaves with Teflon liners. The reactors were tightly sealed and heated to 230 °C for 4 days. After that the autoclaves were cooled down to room temperature at 6 °C h^{-1}. Then the reaction products were isolated by filtration and subsequent several washings with water. Colorless crystals of $NaY(SeO_3)_2$, $KY(SeO_3)_2$, $RbY(SeO_3)_2$, and $CsY(SeO_3)_2$ were obtained in 98%, 99%, 99%, and 90% yields, respectively, on the basis of $Y(NO_3)_3{\cdot}6H_2O$. The reaction products turn out to be pure on the basis of the powder X-ray diffraction (PXRD) (see the PXRD data in Supporting Information). Although every effort has been made using the same synthesis method, it was very difficult to obtain crystals of Li phase.

Single Crystal X-ray Diffraction. Since the structure of $NaY(SeO_3)_2$ has been reported,[35] only the structural characterization of $AY(SeO_3)_2$ (A = K, Rb, and Cs) was carried out. A colorless block with dimension of 0.026 × 0.029 × 0.032 mm^3 for $KY(SeO_3)_2$, a colorless rod with dimension of 0.011 × 0.012 × 0.195 mm^3 for $RbY(SeO_3)_2$, and a colorless octahedron with dimension of 0.025 × 0.032 × 0.045 mm^3 for $CsY(SeO_3)_2$ were utilized for single crystal structure determination. For the data collection, a Bruker SMART BREEZE diffractometer containing a monochromated Mo Kα radiation and a 1K CCD area detector was used at room temperature. A narrow-frame method was used to acquire the data with scan widths of 0.30° in ω and an exposing time of 10 s/frame. The program SAINT was used to integrate the obtained data.[39] The intensities for collected data were corrected for polarization, air absorption, Lorentz factor, and absorption attributed to the deviation through the detector faceplate in the path length. The program SADABS was employed to make a semiempirical absorption correction on the hemisphere of data.[40] The data were solved with SHELXS-97[41,42] and were refined using SHELXL-97.[41,43] The software package WinGX-98 was used for all crystallographic calculations.[44] Crystallographically important data and several selected bond lengths for the reported materials are listed in Tables 1 and 2, respectively.

Table 1. Crystallographic Data for $AY(SeO_3)_2$ (A = K, Rb, and Cs)

	$KYSe_2O_6$	$RbYSe_2O_6$	$CsYSe_2O_6$
fw	381.93	428.30	475.74
space group	*Pnma* (No. 62)	*Pnma* (No. 62)	$Pa\bar{3}$ (No. 205)
a (Å)	13.3838(2)	13.7594(5)	8.8114(2)
b (Å)	5.70270(10)	5.7457(2)	8.8114(2)
c (Å)	8.6759(2)	8.7692(3)	8.8114(2)
V (Å^3)	662.18(2)	693.27(4)	684.12(5)
Z	4	4	4
T (K)	298.0(2)	298.0(2)	298.0(2)
λ (Å)	0.710 73	0.710 73	0.710 73
ρ_{calcd} (g cm^{-3})	3.831	4.103	4.619
μ (mm^{-1})	20.396	25.857	24.379
$R(F)^a$	0.0294	0.0245	0.0148
$R_w(F_o^2)^b$	0.0461	0.0498	0.0383

$^aR(F) = \Sigma ||F_o| - |F_c||/\Sigma |F_o|$. $^bR_w(F_o^2) = [\Sigma w(F_o^2 - F_c^2)^2/\Sigma w(F_o^2)^2]^{1/2}$.

Powder X-ray Diffraction (PXRD). To identify the synthesized materials and to confirm their phase purity, PXRD was used. The PXRD patterns were obtained on a Bruker D8-Advance diffractometer with 40 kV and 40 mA using Cu Kα radiation at RT. The well-ground powdered samples were placed on sample holders, and the XRD data were obtained in the 2θ range 10–70° with a step time of 0.2 s, and a step size of 0.02°. As seen in the Supporting Information, the measured PXRD data are in good agreement with those simulated patterns from the models acquired from single crystal X-ray diffraction.

Infrared Spectroscopy. A Thermo Scientific Nicolet 6700 FT-IR spectrometer was used to record infrared spectra in the spectral range 400–4000 cm^{-1}. The well-ground samples were embedded in KBr matrixes for the measurements.

UV–Vis Diffuse Reflectance Spectroscopy. A Varian Cary 500 scan UV–vis–NIR spectrophotometer at the Korea Photonics Technology Institute was used for obtaining UV–vis diffuse reflectance spectra over the range 200–2500 nm at room temperature. The Kubelka–Munk function was employed to transform the reflectance spectra to the absorbance data.[45,46]

Thermogravimetric Analyses. Thermogravimetric analyses were carried out using a Setaram LABSYS TG-DTA thermogravimetric analyzer. The ground samples were mounted in alumina crucibles, and the temperature was increased to 1000 °C at 10 °C min^{-1} under flowing argon.

Scanning Electron Microscopy/Energy Dispersive Analysis by X-ray (SEM/EDAX). A Hitachi S-3400N and a Horiba Energy EX-250 were used to perform SEM/EDAX. EDAX for $NaY(SeO_3)_2$, $KY(SeO_3)_2$, $RbY(SeO_3)_2$, and $CsY(SeO_3)_2$ reveal approximate A:Y:Se ratio of 1:1:2.

Powder Second-Harmonic Generation (SHG) Measurements. Second-order nonlinear optical properties of NCS $NaY(SeO_3)_2$ were measured by Kurtz-NLO system (1064 nm radiation) using polycrystalline samples.[47] The measurements were performed by a DAWA Q-switched Nd:YAG laser, performing at 20 Hz. Polycrystalline $NaY(SeO_3)_2$ was ground and sieved into different particle size ranges to figure out the type 1 phase matching capability. Ground polycrystalline $NH_4H_2PO_4$ (ADP), $LiNbO_3$, and α-SiO_2 were also sieved into the distinct particle size ranges in order to compare SHG efficiencies relevantly. For comparing SHG efficiencies, samples with particle size range of 45–63 μm were utilized. For the SHG measurements in reflection, the samples containing distinct particle sizes were introduced into separate tubes without using any index-matching fluid. A photomultiplier tube (PMT, Hamamatsu) with a 532 nm narrow-pass interference filter was used to detect only the reflected frequency doubled 532 nm green light. A Tektronix TDS1032 digital oscilloscope was connected to monitor the SHG signal. A comprehensive statement for the equipment and the method employed was reported earlier.[16]

RESULTS AND DISCUSSION

Structures. $NaY(SeO_3)_2$. The crystal structure for $NaY(SeO_3)_2$ has been reported;[35] thus, a concise structural statement will be provided here for comparison. $NaY(SeO_3)_2$ shows the noncentrosymmetric orthorhombic space group, $P2_1cn$ (No. 33). The compound has a three-dimensional framework consisting of YO_7 monocapped trigonal prisms and SeO_3 trigonal pyramids (see Figure 1). The Se^{4+} cations show asymmetric coordination moieties due to the lone pair. The backbone of $NaY(SeO_3)_2$ is composed of zigzag chains of vertex-shared YO_7 polyhedra. The SeO_3 trigonal pyramids work as intra- and interchain connectors and create a 3D backbone. The $Se(1)O_3$ group shares three corners with three Y^{3+} cations and interacts with two Na^+ cations through two oxygen atoms. The $Se(2)O_3$ group shares a corner and an edge with two Y^{3+} cations. Also, two oxygen atoms in $Se(2)O_3$ group contact three Na^+ cations. $NaY(SeO_3)_2$ may be written as an anionic skeletal structure of $\{[Y(1)O_{5/2}O_{2/3}]^{3.333-}\ [Se(1)O_{3/2}]^{1+}\ [Se(2)O_{2/2}O_{1/3}]^{1.333+}\}^-$ in connectivity terms. Overall charge balance is retained by the included Na^+. Bond valence[48,49] for the Y^{3+}, Se^{4+}, Na^+, and O^{2-} is calculated to be 2.98, 4.02, 0.94, and 1.89–2.12, respectively.

$KY(SeO_3)_2$ and $RbY(SeO_3)_2$. The new quaternary alkali metal yttrium selenites, $KY(SeO_3)_2$ and $RbY(SeO_3)_2$, are isostructural and exhibit similar structures to that of NaIn-

dx.doi.org/10.1021/ic500548v | Inorg. Chem. 2014, 53, 4756–4762

Table 2. Selected Bond Distances (Å) for $AY(SeO_3)_2$ (A = K, Rb, and Cs)

$KY(SeO_3)_2$		$RbY(SeO_3)_2$		$CsY(SeO_3)_2$	
Y(1)−O(1) × 2	2.252(3)	Y(1)−O(1) × 2	2.250(3)	Y(1)−O(1) × 6	2.2496(16)
Y(1)−O(2)	2.258(5)	Y(1)−O(2)	2.271(4)	Se(1)−O(1) × 3	1.6900(16)
Y(1)−O(3) × 2	2.265(3)	Y(1)−O(3) × 2	2.260(3)	Cs(1)−O(1) × 6	3.2389(17)
Y(1)−O(4)	2.202(5)	Y(1)−O(4)	2.212(4)	Cs(1)−O(1) × 6	3.4556(17)
Se(1)−O(1) × 2	1.686(3)	Se(1)−O(1) × 2	1.684(3)		
Se(1)−O(2)	1.688(5)	Se(1)−O(2)	1.702(4)		
Se(2)−O(3) × 2	1.688(3)	Se(2)−O(3) × 2	1.691(3)		
Se(2)−O(4)	1.694(5)	Se(2)−O(4)	1.677(4)		
K(1)−O(1) × 2	2.855(3)	Rb(1)−O(1) × 2	2.915(3)		
K(1)−O(2) × 2	3.0190(17)	Rb(1)−O(2) × 2	3.0770(17)		
K(1)−O(3) × 2	2.817(3)	Rb(1)−O(3) × 2	2.920(3)		
K(1)−O(3) × 2	2.828(4)	Rb(1)−O(3) × 2	2.945(3)		

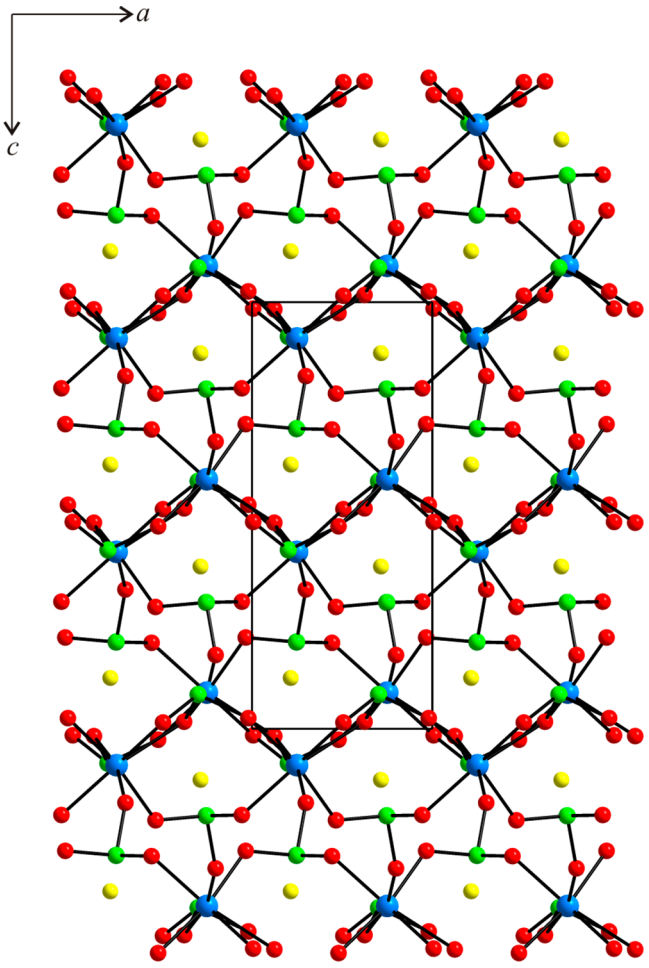

Figure 1. Ball-and-stick model of $NaY(SeO_3)_2$ representing a three-dimensional framework structure in the *ab*-plane (blue, Y; green, Se; yellow, Na; red, O). Note the framework consists of zigzag chains of corner-shared YO_7 polyhedra and SeO_3 linkers.

$(SeO_3)_2$.[50] Thus, only a short structural description of $KY(SeO_3)_2$ will be given here. The structure of $KY(SeO_3)_2$ is considered to be a 3D framework with corner-shared YO_6 octahedra and SeO_3 trigonal pyramids (see Figure 2). Whereas the O−Y−O bond angles vary from 85.77(12)° to 178.02(17)°, the Y−O bond lengths in the distorted YO_6 octahedra vary from 2.202(5) to 2.265(3) Å. In two unique Se^{4+} cations, however, the Se−O bond distances vary from 1.686(3) to 1.694(5) Å. The K^+ cations are in eight-coordinate environment with oxygen atoms, in which the K−O contacts range from 2.817(3) to 3.0190(17) Å. As seen in Figure 2a, each YO_6 octahedron and SeO_3 trigonal pyramid shares their vertices through oxygen and generates a 3D structure. As a result, channels with 4-membered rings (4-MRs) running down to the [001] direction are observed in the *ab*-plane. In the *ac*-plane, 4-(4-MR) and 12-membered ring (12-MR) channels along the [010] direction are also observed (see Figure 2b). Within the 12-MR channels, K^+ cations are residing. Within the 12-MR channels, the lone pairs on the SeO_3 polyhedra are directed toward the inside. Both $Se(1)O_3$ and $Se(2)O_3$ polyhedra share their three corners with three Y^{3+} cations. However, the $Se(1)O_3$ interacts with two K^+ cations through one oxygen atom, and the $Se(2)O_3$ interacts with one K^+ cation with two oxygen atoms. The structural connectivity of $KY(SeO_3)_2$ can be represented as an anionic backbone of $\{[YO_{6/2}]^{3-}$ 2-$[SeO_{3/2}]^{1+}\}^{-}$. The charge balance can be retained by the residing K^+. Bond valence sum calculations[48,49] for the K^+, Se^{4+}, Y^{3+}, and O^{2-} result in values of 1.00, 3.99−4.01, 3.02, and 1.98−2.07, respectively.

$CsY(SeO_3)_2$. $CsY(SeO_3)_2$ is a novel quaternary Cs^+−Y^{3+}−Se^{4+}−oxide that crystallizes in a cubic centrosymmetric space group, $Pa\bar{3}$ (No. 205). $CsY(SeO_3)_2$ exhibits a 3D framework that is composed of YO_6 octahedra and asymmetric SeO_3 groups (see Figure 3). The Y^{3+} is bound to six oxygen in octahedral coordination moiety with O−Y−O bond angles and Y−O bond lengths of 89.05(6)−180.00(11)° and 2.2496(16) Å, respectively. The unique Se^{4+} is connected to three oxygen in SeO_3 group with the observed O−Se−O bond angles of 101.39(7)° and the Se−O bond lengths of 1.6900(16) Å. Finally, 12 oxygen atoms wrap the Cs^+ cation, in which the Cs−O contact distances vary from 3.2389(17) to 3.4556(17) Å. In the center of $CsY(SeO_3)_2$ structure, the Y^{3+} cation forms an octahedron with six oxide ligands (see Figure 3a). The SeO_3 groups then share the vertices of the YO_6 octahedra through the oxygen atoms. As seen in Figure 3b, each oxygen atom in the SeO_3 trigonal pyramids is shared further by the YO_6 octahedra, and the framework spreads out radially, which completes a 3D framework. The lone pairs on SeO_3 that are situated *trans* to each other are directed in opposite directions as expected from the centrosymmetric structure. The SeO_3 group shares its three corners with three Y^{3+} cations and interacts with four Cs^+ cations through three oxygen atoms. Cs^+ cations settle in between the anionic framework to keep the charge neutrality (see Figure 3c). An interesting feature observed in $CsY(SeO_3)_2$ is a highly symmetric cage structure. As can be seen from the inset of Figure 3c, Cs^+ and Y^{3+} cations

dx.doi.org/10.1021/ic500548v | Inorg. Chem. 2014, 53, 4756−4762

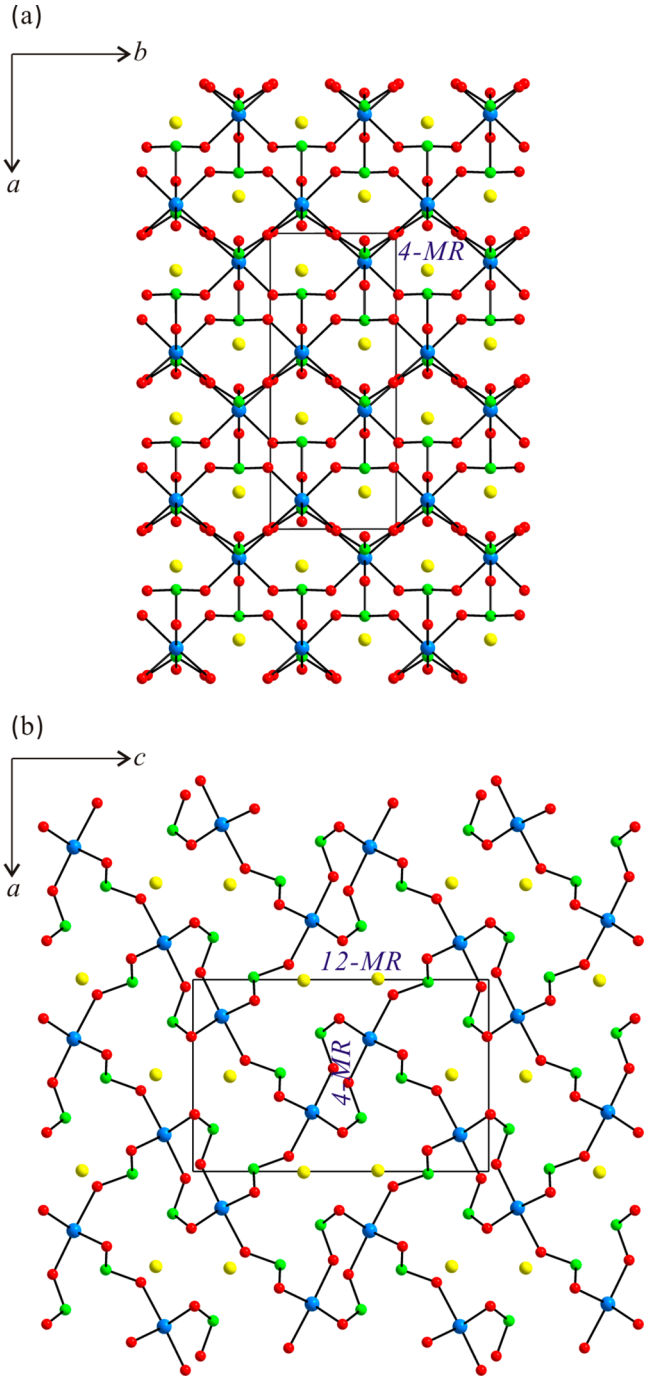

Figure 2. (a) Ball-and-stick model of $KY(SeO_3)_2$ in the *ab*-plane, in which 4-membered ring (4-MR) channels running down the [001] direction are observed. (b) Four-membered ring channels and 12-membered ring channels composed of YO_6 octahedra and SeO_3 polyhedra are observed along the [010] direction in the *ac*-plane (blue, Y; green, Se; yellow, K; red, O).

reside in the center and corners of an octahedron, respectively. When Y^{3+} cations are linked by SeO_3 linkers, an octahedral supercage structure can be obtained. The framework of $CsY(SeO_3)_2$ can be delineated as $\{[YO_{6/2}]^{3-}\ 2[SeO_{3/2}]^{1+}\}^{-}$, and the overall charge is balanced by the Cs^+. Bond-valence[48,49] for the Y^{3+}, Se^{4+}, Cs^+, and O^{2-} can be calculated to be 2.99, 4.03, 0.98, and 2.01, respectively.

Infrared Spectroscopy. Infrared spectra have been obtained to confirm the presence of specific bond networks

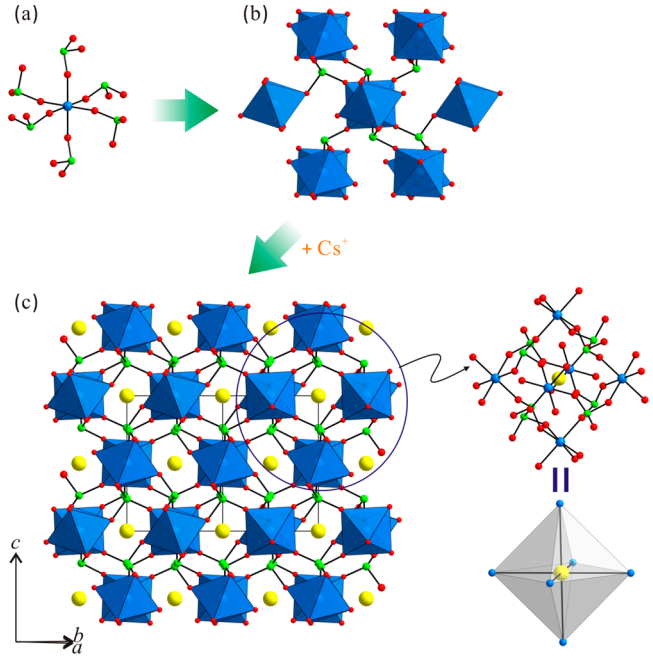

Figure 3. (a) Ball-and-stick model representing a YO_6 octahedron shared by six asymmetric SeO_3 polyhedra in $CsY(SeO_3)_2$ (blue, Y; green, Se; yellow, Cs; red, O). Note the lone pairs on SeO_3 polyhedra located *trans* to each other are directed in opposite directions. Ball-and-stick and polyhedral models showing (b) a radial expansion and (c) a complete three-dimensional framework structure. Note Cs^+ and Y^{3+} cations reside in the center and corners of a highly symmetric octahedral supercage, respectively.

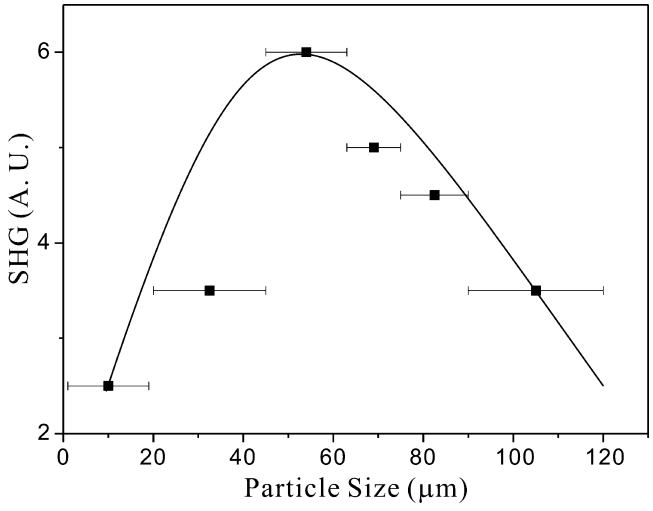

Figure 4. Type 1 phase matching curve for NCS $NaY(SeO_3)_2$. The curve is to guide the eye and is not a fit to the data.

in the reported materials. The infrared spectra for $AY(SeO_3)_2$ (A = Na, K, Rb, or Cs) exhibit both Se−O and Y−O vibrations. While vibrational bands attributable to Y−O are found around 730−870 cm^{-1}, those for Se−O vibrations are found between 463 and 484 cm^{-1}. The assignments are in accordance with those published mixed metal yttrium or selenium oxides.[6,51] The IR spectra for all four materials were deposited in the Supporting Information.

UV−Vis Diffuse Reflectance Spectroscopy. The UV−vis diffuse reflectance spectra of $AY(SeO_3)_2$ have been measured,

dx.doi.org/10.1021/ic500548v | Inorg. Chem. 2014, 53, 4756−4762

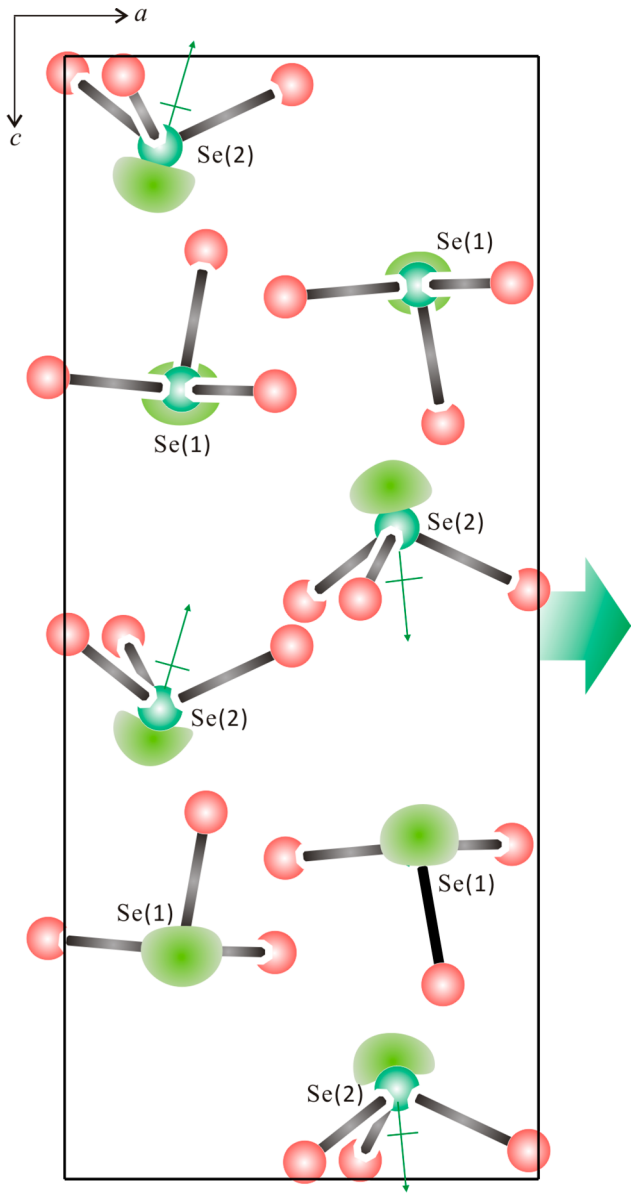

Figure 5. Ball-and-stick model representing the net moment occurring from asymmetric SeO_3 groups in $NaY(SeO_3)_2$. The lone pair on Se^{4+} is drawn schematically and is not the result of the electron localization function (ELF) calculations. When taken as a whole, a small net moment is observed along the [100] direction.

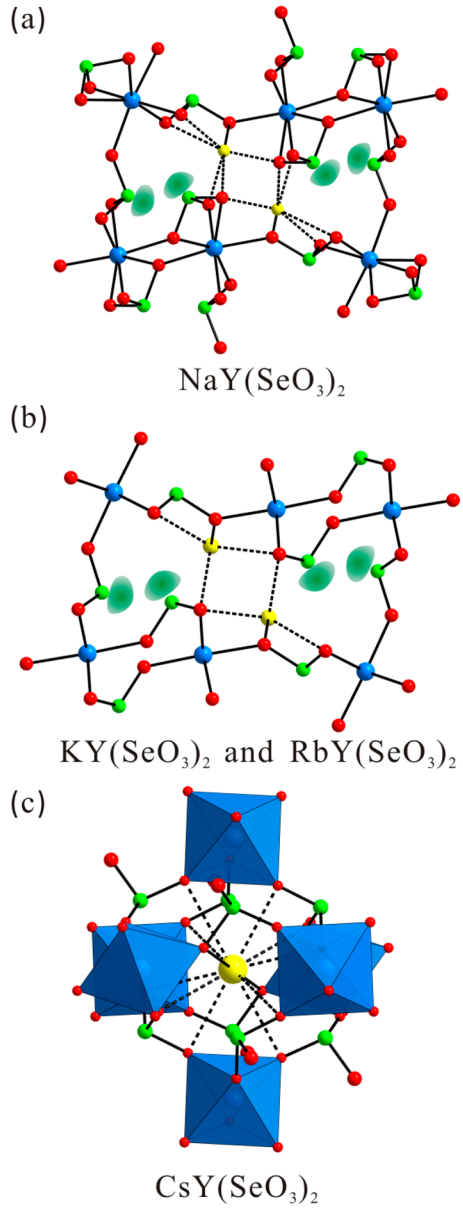

Figure 6. Ball-and-stick and polyhedral models representing how the size and coordination of alkali metal cations influence the framework structures in (a) $NaY(SeO_3)_2$, (b) $AY(SeO_3)_2$ (A = K and Rb), and (c) $CsY(SeO_3)_2$ (blue, Y; green, Se; yellow, Na, K, Rb, or Cs; red, O).

Table 3. Calculation of Dipole Moments for YO_6 and SeO_3 Polyhedra (D = Debyes)

compd	species	dipole moment (D)
$NaY(SeO_3)_2$	$Se(1)O_3$	7.27
	$Se(2)O_3$	8.07
$KY(SeO_3)_2$	$Y(1)O_6$	1.82
	$Se(1)O_3$	7.43
	$Se(2)O_3$	7.45
$RbY(SeO_3)_2$	$Y(1)O_6$	0.70
	$Se(1)O_3$	7.20
	$Se(2)O_3$	7.64
$CsY(SeO_3)_2$	$Y(1)O_6$	0
	$Se(1)O_3$	7.49

and the following Kubelka–Munk function has been used to calculate the absorption (K/S) data:[45,46]

$$F(R) = \frac{(1-R)^2}{2R} = \frac{K}{S}$$

Here, S is the scattering, R represents the reflectance, and K denotes the absorption. From the (K/S)-versus-E plots, band gaps for $NaY(SeO_3)_2$, $KY(SeO_3)_2$, $RbY(SeO_3)_2$, and $CsY(SeO_3)_2$ are extracted to be 4.6, 4.9, 4.4, and 4.4 eV, respectively, by extrapolating the linear parts of the ascending curves to zero. The obtained band gaps seem to be attributed to the distortions originated from SeO_3 polyhedra and the extent of Y (4d) orbitals engaged in the conduction bands. The UV–vis diffuse reflectance spectra for all four reported materials were added in the Supporting Information.

dx.doi.org/10.1021/ic500548v | Inorg. Chem. 2014, 53, 4756–4762

Thermal Analysis. The thermal behaviors for $AY(SeO_3)_2$ (A = Na, K, Rb, and Cs) were examined using thermogravimetric analyses. Both $KY(SeO_3)_2$ and $RbY(SeO_3)_2$ reveal thermal stabilities up to 620 °C, whereas $NaY(SeO_3)_2$ and $CsY(SeO_3)_2$ are stable to 570 °C on the basis of TGA diagrams. Above the temperatures, however, the materials decompose due to the sublimation of SeO_2. Mixtures of Y_2O_3 and corresponding alkali metal selenium oxides, A_2SeO_4 (A = Na, K, Rb, and Cs),[52−55] are confirmed by PXRD of thermal decomposition products for $AY(SeO_3)_2$ at 1000 °C in air.

Second-Order Nonlinear Optical (NLO) Measurements. As mentioned earlier, $NaY(SeO_3)_2$ exhibits an NCS structure; thus, the detailed SHG characteristics were studied. Powder NLO measurements with 1064 nm radiation reveal that $NaY(SeO_3)_2$ possesses a similar SHG intensity to that of $NH_4H_2PO_4$ (ADP). To decide the phase-matching (type 1) features of $NaY(SeO_3)_2$, additional SHG measurements on the sieved polycrystalline $NaY(SeO_3)_2$ into several distinct particle sizes have been performed. As can be seen in Figure 4, $NaY(SeO_3)_2$ is classified as a class C SHG material (non-phase-matchable).[47]

The observed SHG efficiency for $NaY(SeO_3)_2$ can be explained once the net polarization direction arising from the constituent noncentrosymmetric polyhedra is analyzed. In an asymmetric unit, two unique Se^{4+} cations exist as can be seen in Figure 5. The lone pairs on $Se(1)^{4+}$ are approximately directed to the [01−1], [0−1−1], [0−11], and [011] directions; thus, the polarization associated with $Se(1)^{4+}$ almost cancels. However, the lone pairs on $Se(2)^{4+}$ point almost to the [−101] and [−10−1] directions, although the polyhedra are slightly tilted along the *b*-direction. One can clearly find a 2_1 screw axis along the *a*-axis as expected from the space group of $NaY(SeO_3)_2$. With $Se(2)^{4+}$ cations, when taken as a whole, a small net moment can be found directing to the [100] direction, which is responsible for the SHG efficiency of $NaY(SeO_3)_2$ (see Figure 5).

Dipole Moment Calculations. Although not all four reported materials crystallize in macroscopic NCS space groups, they do contain polyhedra of distorted coordination environment such as YO_6 and SeO_3. Thus, more detailed investigation on the degree of distortions in the constituent polyhedra would be necessary in order to understand the coordination environments better. One nice approach quantifying the magnitude and direction of the distortions is to determine the local dipole moments of the asymmetric polyhedra.[56−58] The method utilizes a bond valence sum for the calculations. The dipole moments for the YO_6 and SeO_3 polyhedra can be calculated to be 0−1.82 and 7.20−8.07 D (D = Debyes) using this methodology. The values for SeO_3 groups are in accordance with those previously published dipole moments.[34,59,60] A list of calculated dipole moments for the YO_6 and SeO_3 polyhedra is summarized in Table 3.

Cation Size versus Framework Structures. Although the stoichiometry of four reported alkali metal yttrium selenium oxide materials, $AY(SeO_3)_2$ (A = Na, K, Rb, and Cs), are similar, they exhibit different bonding networks depending on the involved alkali metal cations. Whereas $NaY(SeO_3)_2$ contains zigzag chains of corner-shared YO_7 polyhedra and SeO_3 linkers, $KY(SeO_3)_2$ and $RbY(SeO_3)_2$ exhibit channels with corner-shared YO_6 octahedra and SeO_3 trigonal pyramids. Besides, $CsY(SeO_3)_2$ reveals highly symmetric octahedral supercages that are composed of YO_6 octahedra, SeO_3 polyhedra, and Cs^+ cations. More close examinations on the structures of $AY(SeO_3)_2$ suggest that the dimension and coordination environment of the alkali metal cations influence significantly the architecture of the backbone. In $NaY(SeO_3)_2$, smaller Na^+ (1.06 Å)[61] cations interact strongly with oxygen atoms within the channel (see Figure 6a). In fact, the 10-MR channel containing Na^+ and lone pairs on Se^{4+} is very crowded. In order to maintain channel structure within a packed space, YO_7 polyhedra share their edges. Also, relatively stronger interaction of Na^+ cations with oxygen atoms directs the locations of SeO_3 polyhedra within a limited space, which makes $NaY(SeO_3)_2$ crystallize in a NCS space group. In $KY(SeO_3)_2$ and $RbY(SeO_3)_2$, larger K^+ (1.38 Å) or Rb^+ (1.52 Å) cations reside in the channel interacting with oxygen atoms (see Figure 6b). Larger channels of $KY(SeO_3)_2$ and $RbY(SeO_3)_2$ have more room compared to that of $NaY(SeO_3)_2$ attributable to their greater cation sizes. However, YO_6 and SeO_3 polyhedra in $KY(SeO_3)_2$ and $RbY(SeO_3)_2$ share their corners and form 12-MR channels in order to maintain the frameworks. In $CsY(SeO_3)_2$, huge Cs^+ (1.88 Å) cations interact with 12 oxygen atoms. Thus, the 10-MR or 12-MR channel structures observed in $AY(SeO_3)_2$ (A = Na, K, and Rb) cannot be maintained. Instead, cages containing bulky cations inside are produced, and the stereoactive lone pairs on SeO_3 are pointed *trans* to each other (see Figure 6c).

■ CONCLUSIONS

Four new alkali metal yttrium selenium oxides, $AY(SeO_3)_2$ (A = Na, K, Rb, and Cs), were synthesized through hydrothermal reactions. Although the reported materials reveal 3D frameworks, they have different crystal structures. $NaY(SeO_3)_2$ reveals 10-MR channels, $KY(SeO_3)_2$ and $RbY(SeO_3)_2$ exhibit 12-MR channels, and $CsY(SeO_3)_2$ shows cages in their framework structures. The structural variations and different space groups for the reported compounds seem to be due to the alkali metals' dimension and coordination environment. Powder NLO tests on NCS $NaY(SeO_3)_2$ reveal that the compound has a similar SHG efficiency to that of $NH_4H_2PO_4$. Detailed structural analysis suggests the observed SHG is responsible for a net moment originating from the lone pair cation, Se^{4+}. Further characterization including thermal analyses, SEM/EDAX, infrared and UV−vis diffuse reflectance spectroscopies, and dipole moment calculations have also been successfully presented.

■ ASSOCIATED CONTENT

Supporting Information

X-ray crystallographic file in CIF format, calculated and observed X-ray diffraction patterns, thermogravimetric analysis diagrams, infrared spectra, and UV−vis diffuse reflectance spectra for $AY(SeO_3)_2$ (A = Na, K, Rb, and Cs). This material is available free of charge via the Internet at http://pubs.acs.org.

■ AUTHOR INFORMATION

Corresponding Author

*E-mail: kmok@cau.ac.kr. Phone: +82-2-820-5197. Fax: +82-2-825-4736.

Notes

The authors declare no competing financial interest.

■ ACKNOWLEDGMENTS

This research was supported by Basic Science Research Program through the National Research Foundation of Korea

(NRF) funded by Ministry of Education, Science & Technology (Grant 2013R1A2A2A01007170). This research was also supported by the Chung-Ang University Freshmen Academic Record Excellent Scholarship Grants in 2014 (for S.-e.B.).

REFERENCES

(1) Lide, D. R. *CRC Handbook of Chemistry and Physics, Internet Version 2005*; CRC Press: Boca Raton, FL, 2005.
(2) Ok, K. M.; Halasyamani, P. S. *Chem. Mater.* **2002**, *14*, 2360−2364.
(3) Shen, Y. L.; Jiang, H. L.; Xu, J.; Mao, J.-G.; Cheah, K. W. *Inorg. Chem.* **2005**, *44*, 9314−9321.
(4) Harrison, W. T. A.; Dussack, L. L.; Jacobson, A. J. *Inorg. Chem.* **1994**, *33*, 6043−6049.
(5) Vaughey, J. T.; Harrison, W. T. A.; Dussack, L. L.; Jacobson, A. J. *Inorg. Chem.* **1994**, *33*, 4370−4375.
(6) Porter, Y.; Halasyamani, P. S. *J. Solid State Chem.* **2003**, *174*, 441−449.
(7) Sivakumar, T.; Chang, H. Y.; Baek, J.; Halasyamani, P. S. *Chem. Mater.* **2007**, *19*, 4710−4715.
(8) Jiang, H.; Kong, F.; Fan, Y.; Mao, J.-G. *Inorg. Chem.* **2008**, *47*, 7430−7437.
(9) Chang, H. Y.; Kim, S. W.; Halasyamani, P. S. *Chem. Mater.* **2010**, *22*, 3241−3250.
(10) Li, P.-X.; Zhang, S.-Y.; Mao, J.-G. *Dalton Trans.* **2010**, *39*, 11560−11567.
(11) Oh, S.-J.; Lee, D. W.; Ok, K. M. *Inorg. Chem.* **2012**, *51*, 5393−5399.
(12) Oh, S.-J.; Lee, D. W.; Ok, K. M. *Dalton Trans.* **2012**, *41*, 2995−3000.
(13) Jona, F.; Shirane, G. *Ferroelectric Crystals*; Pergamon Press: Oxford, U.K., 1962.
(14) Cady, W. G. *Piezoelectricity; an Introduction to the Theory and Applications of Electromechanical Phenomena in Crystals*; Dover: New York, 1964; p 822.
(15) Lang, S. B. *Sourcebook of Pyroelectricity*; Gordon & Breach Science: London, 1974.
(16) Ok, K. M.; Chi, E. O.; Halasyamani, P. S. *Chem. Soc. Rev.* **2006**, *35*, 710−717.
(17) Opik, U.; Pryce, M. H. L. *Proc. R. Soc. London* **1957**, *A238*, 425−447.
(18) Bader, R. F. W. *Mol. Phys.* **1960**, *3*, 137−151.
(19) Pearson, R. G. *THEOCHEM* **1983**, *103*, 25−34.
(20) Wheeler, R. A.; Whangbo, M.-H.; Hughbanks, T.; Hoffmann, R.; Burdett, J. K.; Albright, T. A. *J. Am. Chem. Soc.* **1986**, *108*, 2222−2236.
(21) Ra, H.-S.; Ok, K. M.; Halasyamani, P. S. *J. Am. Chem. Soc.* **2003**, *125*, 7764−7765.
(22) Kim, Y. H.; Lee, D. W.; Ok, K. M. *Inorg. Chem.* **2013**, *52*, 11450−11456.
(23) Kim, Y. H.; Lee, D. W.; Ok, K. M. *Inorg. Chem.* **2014**, *53*, 1250−1256.
(24) Zhang, D.; Johnsson, M. *Acta Crystallogr., Sect. E* **2008**, *64*, i26/1−i26/6.
(25) Lee, D. W.; Kim, S. B.; Ok, K. M. *Dalton Trans.* **2012**, *41*, 8348−8353.
(26) Chen, C. T.; Ye, N.; Lin, J.; Jiang, J.; Zeng, W. R.; Wu, B. C. *Adv. Mater.* **1999**, *11*, 1071−1078.
(27) Pan, S.; Smit, J. P.; Watkins, B.; Marvel, M. R.; Stern, C. L.; Poeppelmeier, K. R. *J. Am. Chem. Soc.* **2006**, *128*, 11631−11634.
(28) Wu, H. P.; Pan, S. L.; Poeppelmeier, K. R.; Li, H. Y.; Jia, D. Z.; Chen, Z. H.; Fan, X. Y.; Yang, Y.; Rondinelli, J. M.; Luo, H. S. *J. Am. Chem. Soc.* **2011**, *133*, 7786−7790.
(29) Sykora, R. E.; Ok, K. M.; Halasyamani, P. S.; Albrecht-Schmitt, T. E. *J. Am. Chem. Soc.* **2002**, *124*, 1951−1975.
(30) Goodey, J.; Ok, K. M.; Broussard, J.; Hofmann, C.; Escobedo, F. V.; Halasyamani, P. S. *J. Solid State Chem.* **2003**, *175*, 3−12.
(31) Ok, K. M.; Baek, J.; Halasyamani, P. S.; O'Hare, D. *Inorg. Chem.* **2006**, *45*, 10207−10214.
(32) Choi, M.-H.; Kim, S.-H.; Chang, H. Y.; Halasyamani, P. S.; Ok, K. M. *Inorg. Chem.* **2009**, *48*, 8376−8382.
(33) Lee, D. W.; Bak, D.-b.; Kim, S. B.; Kim, J.; Ok, K. M. *Inorg. Chem.* **2012**, *51*, 7844−7850.
(34) Lee, D. W.; Ok, K. M. *Inorg. Chem.* **2013**, *52*, 5176−5184.
(35) Morris, R. E.; Hriljac, J. A.; Cheetham, A. K. *Acta Crystallogr., Sect. C* **1990**, *62*, 2013−2017.
(36) Harrison, W. T. A. *Acta Crystallogr., Sect. E* **2006**, *62*, i152−i154.
(37) Lipp, C.; Schleid, T. *Z. Anorg. Allg. Chem.* **2008**, *634*, 657−661.
(38) Bang, S.-e.; Pan, Z.; Kim, Y. H.; Lee, D. W.; Ok, K. M. *J. Solid State Chem.* **2013**, *208*, 65−70.
(39) *SAINT, Program for Area Detector Absorption Correction; Version 4.05*; Siemens Analytical X-ray Instruments: Madison, WI, 1995.
(40) Blessing, R. H. *Acta Crystallogr., Sect. A* **1995**, *51*, 33−38.
(41) Sheldrick, G. M. *Acta Crystallogr., Sect. A* **2008**, *64*, 112−122.
(42) Sheldrick, G. M. *SHELXS-97—A Program for Automatic Solution of Crystal Structures*; University of Goettingen: Goettingen, Germany, 1997.
(43) Sheldrick, G. M. *SHELXL-97—A Program for Crystal Structure Refinement*; University of Goettingen: Goettingen, Germany, 1997.
(44) Farrugia, L. J. *J. Appl. Crystallogr.* **1999**, *32*, 837−838.
(45) Kubelka, P.; Munk, F. *Z. Tech. Phys.* **1931**, *12*, 593.
(46) Tauc, J. *Mater. Res. Bull.* **1970**, *5*, 721−729.
(47) Kurtz, S. K.; Perry, T. T. *J. Appl. Phys.* **1968**, *39*, 3798−3813.
(48) Brown, I. D.; Altermatt, D. *Acta Crystallogr., Sect. B* **1985**, *41*, 244−247.
(49) Brese, N. E.; O'Keeffe, M. *Acta Crystallogr., Sect. B* **1991**, *47*, 192−197.
(50) Lee, D. W.; Kim, S. B.; Ok, K. M. *Inorg. Chem.* **2012**, *51*, 8530−8537.
(51) Raju, K. V.; Raju, C. N.; Sailaja, S.; Dhoble, S. J.; Reddy, B. S. *J. Lumin.* **2013**, *134*, 297−302.
(52) Kálmán, A.; Cruickshank, D. W. J. *Acta Crystallogr., Sect. B* **1970**, *26*, 436.
(53) Kálmán, A.; Stephens, J. S.; Cruickshank, D. W. J. *Acta Crystallogr., Sect. B* **1970**, *26*, 1451−1454.
(54) Takahashi, I.; Onodera, A.; Shiozaki, Y. *Acta Crystallogr., Sect. C* **1987**, *43*, 179−182.
(55) Zuniga, F. J.; Breczewski, T.; Arnaiz, A. *Acta Crystallogr., Sect. C* **1991**, *47*, 638−640.
(56) Galy, J.; Meunier, G. *J. Solid State Chem.* **1975**, *13*, 142−159.
(57) Maggard, P. A.; Nault, T. S.; Stern, C. L.; Poeppelmeier, K. R. *J. Solid State Chem.* **2003**, *175*, 27−33.
(58) Izumi, H. K.; Kirsch, J. E.; Stern, C. L.; Poeppelmeier, K. R. *Inorg. Chem.* **2005**, *44*, 884−895.
(59) Lee, D. W.; Ok, K. M. *Solid State Sci.* **2010**, *12*, 2036−2041.
(60) Lee, D. W.; Oh, S. J.; Halasyamani, P. S.; Ok, K. M. *Inorg. Chem.* **2011**, *50*, 4473−4480.
(61) Shannon, R. D. *Acta Crystallogr., Sect. A* **1976**, *32*, 751−767.